Formation of graphene and hexagonal boron nitride on Rh(111) studied by in-situ scanning tunneling microscopy

Dong, G.

Chapter 11 Growth kinetics

11.1 Introduction

Chemical vapor deposition (CVD) of hydrocarbon molecules on transition metals (TMs) provides a practical method for graphene production [25, 51-58, 99]. Detailed insight in the basic steps of the growth process of graphene will prove essential for developing procedures for the production of high-quality graphene. In order to acquire such insight, direct observations and measurements at the elevated process temperatures would be very helpful. Based on more traditional measurements after cool-down of graphene samples, it is difficult to reconstruct the processes that have taken place at high temperature. However, it is technically challenging to perform atomic-scale observations at high temperatures, and because of this difficulty, only a few reports exist of this type. Using low energy electron microscopy (LEEM), McCarty *et al.* [51, 53, 98] have performed some wonderful, *in-situ* work. They have investigated the growth of graphene from various sources, i.e. CVD, sublimation, segregation on Ru and Ir. One of the important conclusions from that work is that graphene growth is fed by the supersaturated, two-dimensional gas of C adatoms rather than by direct exchange between the C dissolved in the substrate and the graphene. The growth speed of the graphene v scales nonlinearly with the concentration of carbon adatoms C on the metal surface, according to

$$v \propto \left[\left(\frac{C}{C^{eq}}\right)^{n} - 1\right] \qquad \text{Eq. 11.1}$$

where n=5 and C^{eq} is the equilibrium density of carbon with respect to the graphene islands. The growth speed was equated to $v = \frac{1}{\mathrm{L}}\mathrm{d}A/\mathrm{d}t$, where A and L are the area and perimeter of a graphene island or of a bare region of the metal substrate that is enclosed by growing graphene. The temperature-independent value of 5 for n was interpreted as

an indication that five carbon atoms are needed to form a cluster, before they can be incorporated into the graphene structure.

In this chapter, we use high-temperature scanning tunneling microscope (STM) movies to reveal the microscopic details of the growth kinetics of graphene on Rh(111). Clear evidence will be provided that on this surface the growth proceeds in unit cells of the moiré pattern between the overlayer and the substrate, which are much larger than a 5-atom C cluster. We continue to show that the addition of moiré unit cells that involve the creation of new kinks is associated with a higher energy barrier than the advancement of a kink position. Kink creation has lower barrier at a concave corner in the graphene than on a straight edge, which makes the growth speed of graphene much faster at the inner contour of a graphene vacancy island than at the outer contour of a compact graphene island. We also show that the rate at which new kinks are created at a concave corner depends on the corner angle.

All measurements were performed in an ultrahigh vacuum (UHV) system with a variable-temperature STM (prototype of the commercial VT-STM of Leiden Probe Microscopy BV). [33, 34]. The base pressure of the system was 4 x 10^{-11} mbar. Sample temperatures were measured by a K-type thermocouple, spot-welded directly onto the Rh single crystal. Gas pressures were measured by an ionization gauge. The sensitivity of the ionization gauge for ethylene of 2.3, relative to that for N_2, is taken into account in all reported pressure values. The clean Rh(111) surface [73] was exposed to 1.3 x 10^{-5} mbar s of ethylene at room temperature, and was heated to 975 K. Graphene islands were formed on the surface with a density suitable for further *in-situ* STM measurements. On this graphene-seeded surface, which was held at 975 K throughout the rest of the experiment, STM images were recorded continuously over a period of 76 minutes, while the surface was exposed to further ethylene at pressures increasing from 1.3 × 10^{-10} to 1.5 ×10^{-8} mbar. The entire STM movie can be found online [100]. For this chapter, we have analyzed three selected episodes from the STM movie, during which the ethylene pressure was at a constant value of 5.7 x 10^{-9} mbar. The STM images at the start and end of each of the three episodes are shown in Fig. 11.1. In this chapter, we report images and quantitative data extracted from a single movie, but note that we have repeated the procedure several times, each time with fully equivalent results.

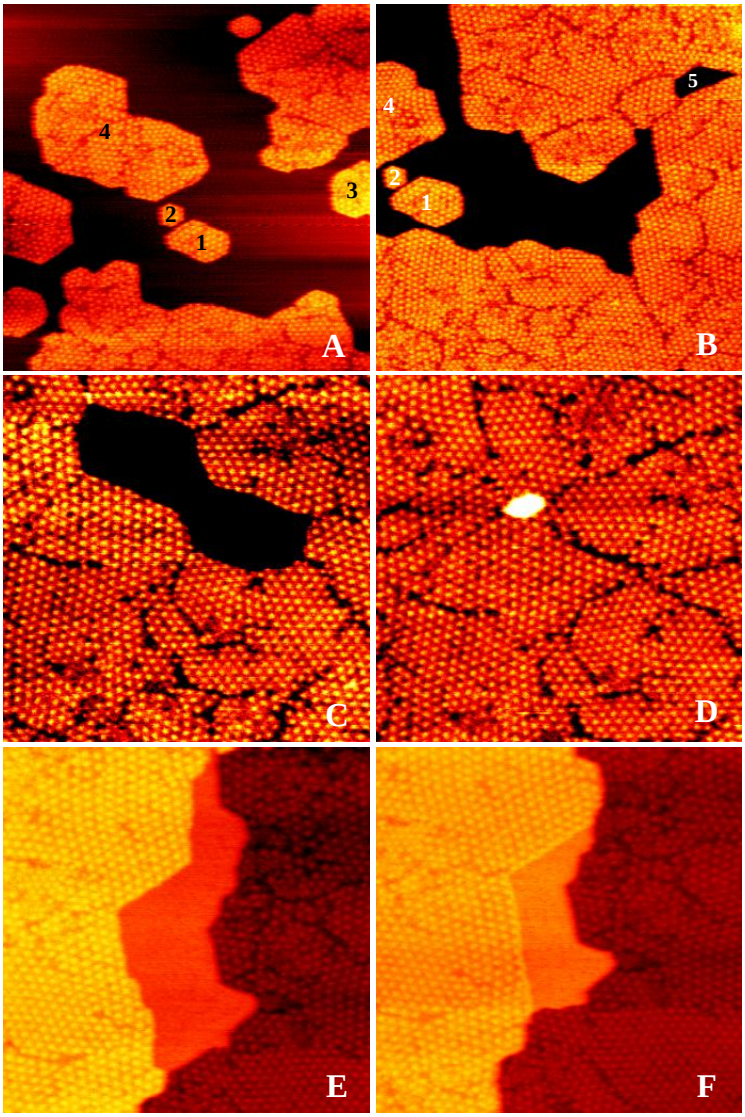

Fig. 11.1 Six snapshots from an STM movie [100], during the growth of graphene at 975 K on a graphene-seeded Rh(111) substrate at a constant ethylene pressure of 5.7 x 10^{-9} mbar. Frame to frame analysis was performed for the 865 s period between panels A and B, the 524 s period between C and D, and the 236 s period between E and F. The average edge advancement rates the 4 graphene islands and 1 vacancy island in A and B (labeled 1 to 5) are discussed in the text.
All images were taken at a sample voltage of V_b = -1.84 V and a tunneling current of I_t = 0.05 nA. The image sizes are 160 x 160 nm^2 for panels A and B and 100 x 100 nm^2 for panels C to F.

11.2 How the moiré pattern influences the growth

Fig. 11.2 (A-C) shows three subsequent STM images from the movie [101]. The structure that is clearly visible is the 2.9 nm moiré pattern between the aligned lattices of the graphene and the Rh. What is demonstrated by Fig. 11.2 and is observed throughout the entire movie is that the advancement of the edges appears to proceed stepwise, in units of this moiré lattice. Entire rows of such units are added. Also within the rows, the growth appears to proceed in moiré units. It starts along an edge by the creation of a new kink (or kink pair), which has a width that corresponds to the full period of the moiré lattice. After this, the new kink rapidly progresses along the edge, moving by single or multiple moiré units from image to image. This growth in moiré lattice units (288 C atoms when the graphene lattice is aligned with the Rh lattice) is reminiscent of the growth of hexagonal boron nitride on Rh(111) [20]. The rate-limiting step in the formation of a single moiré unit most probably does not involve the simultaneous arrival of 288 atoms. Otherwise, the growth rate should be exceptionally non-linear with respect to the ethylene pressure, which is in conflict with our observations and with the n=5 of ref. [98]. This contradiction is resolved by a growth scenario, in which C edge adatoms first need to form a cluster of a certain critical size, e.g. 5, after which the remainder of the moiré unit is formed rapidly. If this is indeed the case, it should be possible to observe intermediate configurations with incomplete moiré lattice units. Indeed, occasionally such configurations were observed, as is illustrated by Fig. 11.2D. Recent theoretical work [102] predicted that the lattice mismatch between graphene and the metal substrate influences the growth of graphene, which is now confirmed by this observation. In energy terms this implies that the energy landscape is modulated by the moiré structure: the lowest-free-energy configuration is that of an integer number of moiré units and the maximum-free-energy configuration is one in which a small number of atoms is added to that. Further addition of atoms lowers the free energy until the full 288 atoms have been added to complete the next moiré unit and the free energy is at a minimum again. The growth is then modulated in large, moiré units, but the critical nucleus is microscopic. The microscopic stable size can be 5 C atoms [98], or 24 C atoms (7 C_6 rings) as suggested by Wang *et al*. [103], and it can be different at various growth sites e.g. straight edges, corners, as discussed below. In this scenario, Eq.11.1 is still satisfied.

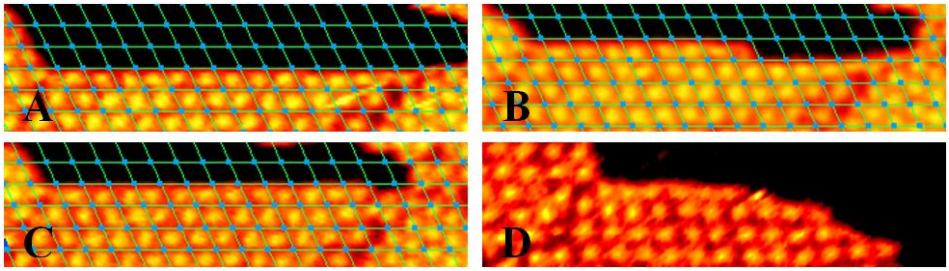

Fig. 11.2 Four snapshots from an STM movie [101], during graphene growth at 975 K on graphene-seeded Rh(111) at an ethylene pressure of 5.7 x 10^{-9} mbar. (A) – (C) are subsequent images (26.2 s each) of a graphene edge, starting out straight in (A), showing a kink in (B), which has advanced to the right in (C), all changes discretized in units of the moiré pattern. Panel (D) shows an incomplete moiré unit, as we observed occasionally. The grids in the image indicate the moiré pattern between graphene and the substrate. Image size: 55 x 15 nm^2. Sample voltage: -1.84 V. Tunneling current: 50 pA.
All images were taken at a sample voltage of V_b = -1.84 V and a tunneling current of I_t = 0.05 nA. The image sizes are 55 x 15 nm^2.

In order to quantify the growth, we separate the process into two stages: kink creation and kink advancement, as shown in Fig. 11.3A. The former introduces one or more new kinks and the latter merely advances the position of an existing kink. Here we discuss direct measurements of the rates of kink formation, both on edges and at corners of the graphene overlayer and the rate of kink advancement. On internal edges of graphene vacancy islands, the creation and advancement of kinks was readily observed using STM, as shown in Fig. 11.2. On external edges of graphene patches we have hardly observed any kink; in most cases we could only observe the sudden addition of a complete row with the width of one unit cell of the moiré lattice. So, we derive the advancement rate from internal edges and use the row addition rate to get the kink formation rate. We restrict the analysis of kink formation at corners and of kink advancement to a single vacancy island (Fig. 11.1E to F) and to a limited time window, within which the change in geometry and the change in bulk C contribution (segregation) could at most have been very modest, which should result in a negligible variation in C adatom density on the metal surface. The advancement of a kink was measured to proceed at a rate of 1230 C atoms per image (26.2 s acquisition time per frame) with a surprisingly high standard deviation of 580 C atoms. If the kink were to advance by uncorrelated single-atom events, the standard deviation should have been $\sqrt{1230} = 35$.

The strong statistical variation indicates that the growth proceeds in units that are much larger than a single C atom or a 5-atom cluster, namely in units that are as large as $(580/35)^2 = 270$ atoms, fully consistent with a growth unit of 1 moiré unit cell (288 atoms). This indicates that graphene growth proceeds by the advancement of kinks that not only have a width of one complete moiré unit, but also advance effectively in steps of single moiré units.

The creation rate of new kinks at corners was found to depend on the corner angle, as shown in Fig. 11.3B. The maximum of 2 kinks/frame was still lower than the kink advancement rate of 4.3 moiré units/frame. The kink creation rate measured at the same ethylene pressure at straight edges was dramatically lower, namely 1.4 x 10^{-4} units/site/frame. Most kink creation events on straight edges were observed to take place at domain boundaries. We conclude that the creation of new kinks is the rate-limiting step and that this is easiest at concave corners. Even though this conclusion of growth by kink formation and advancement seems consistent with previous work [51, 98, 104], we should bare in mind that the kinks in the moiré pattern, discussed here, are much larger than the single graphene unit-cell kinks considered before.

The fact that the growth of graphene takes place at kinks in the moiré pattern should be reflected in the statistical variations in the filling rate of a graphene vacancy islands. This idea is tested in Fig. 4B, where we have plotted the time dependence of the difference in vacancy island area between subsequent frames (episode between panels C-D in Fig. 2). Below, we will discuss why this vacancy island fills up more or less exponentially with time. Fig. 11.4B shows that the filling up of the vacancy island displays significant variations, beyond the inaccuracies in the STM measurement. For example, in the first 250 seconds in Fig. 4B, the average number of C atoms added in the vacancy island between subsequent STM images is $N = 1910$, with a standard deviation of $\Delta N^{exp} = 1360$ C atoms. The experimental inaccuracy on N is no more than $\Delta N^{error} = 510$ C atoms. The extra variation $\Delta N = \sqrt{(\Delta N^{exp})^2 - (\Delta N^{error})^2}$ amounts to 1260 C atoms, which is a factor 29 larger than the expected number of $\sqrt{N}$, deriving from atom-by-atom statistics. This appears to support the notion that the effective growth unit is significantly larger than a single atom. However, assuming graphene to grow by building blocks of B C atoms, we expect the statistical fluctuation to be $\Delta N/N = 1/\sqrt{(N/B)}$, from which we obtain an estimate of $B = 840$ C atoms. This number is not only much larger than the 5-

atom unit of ref. [98], but also larger than the 288 C-atom size of the unit cell of the moiré pattern of graphene on Rh(111). We can easily understand this by realizing that growth only takes place at kink sites, the number of which K is also subject to statistical variations. The combined effect on the fluctuation in the number of atoms added between subsequent images is expressed by $\Delta N = \sqrt{(Rt\Delta K)^2 + (\Delta(Rt)\sqrt{K})^2}$. Here, R stands for the average rate at which C atoms attach to each kink, t is the time between images, and K is the average number of kinks within the inner contour of the vacancy island. Expressed in these quantities, $N = RtK$. The the first term in the square root derives from the fluctuations in the number of kinks, while the second term represents the combination of the independent fluctuations in the advancement of K kinks. Both from individual images and from the ratio between the total filling rate and the observed advancement rate of single kinks we derive the same average number of kinks in the vacancy island of Fig. 11.1C and D of $K = 1.6$. Substituting this together with the measured values for Rt and $\Delta(Rt)$ in the expression for ΔN, we obtain an expected value for this fluctuation of 1700, which agrees reasonably well with the measured value of $\Delta N = 1260$. Note, that the main contribution to the statistical fluctuations in the filling rate result from the variation in the number of kinks.

Here we have concentrated on graphene regions that were aligned relatively well with respect to the Rh substrate. The orientation and period of the moiré pattern depends sensitively on the relative orientation of the graphene and the substrate. Also the energetic preference for forming complete moiré unit cells should be expected to depend significantly on the orientation. These aspects may influence the growth in a very complex way. Further experiments and theory are required to explore this in detail.

11.3 The influence of corner structure on kink creation

Our STM movies show that kinks are preferably created at corners and we already argued that this is because at concave corners the addition of a new moiré unit introduces only a single kink. The first image of a new kink usually shows it as either one

unit of the moiré pattern or a short row of such units, emanating from a corner. The further addition of moiré units does not involve extra kinks, which makes that a lower-energy process. In other words, the creation of new kinks is the rate-limiting step and this is easiest at concave corners. We now inspect the effect of the corner structure, in particular the corner angle, on the kink creation rate. In order to exclude systematic differences in our analysis, we only compared kink creation rates at the contour of a single enclosed Rh region, namely the one shown in Fig. 11.1E and F. Within this region, at each point in time the carbon adatom density must have been close to uniform, so that the corners in the contour experienced very similar supplies of carbon. In Fig. 11.3B, the dependence of the rate of kink creation on the angle of the graphene corner is shown, as was counted from the kink creation events recorded for each of six selected corners with different angles in the contour of the Rh region in Fig. 11.1E and F. The error margins reflect the limited number of in total 27 kink creation events that were counted. Fig. 11.3B shows that it is very difficult to create a kink at a corner with an opening angle larger than 120º and it suggests that there is a significant preference for kink formation at a 60º corner, which is a natural angle for the lattice of the graphene and that of the moiré pattern.

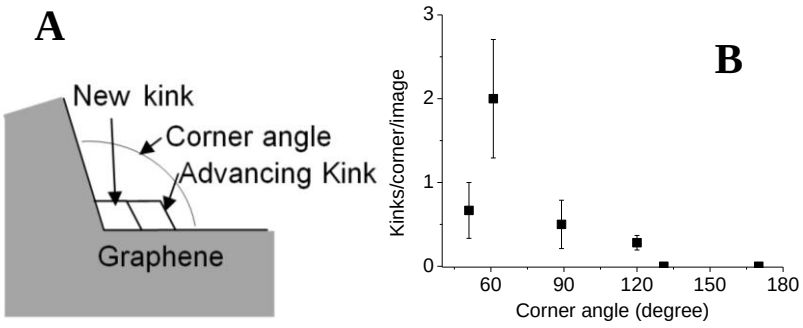

Fig. 11.3 (A) Sketch of kink creation at a concave graphene corner and subsequent kink advancement. The nucleation and growth units correspond to complete unit cells of the moiré pattern. Note that a new kink introduces two extra corners (one concave and one convex), whereas the advancement does not require the creation of further corners. (B) The measured average number of kink creation events per STM image as a function of the angle of the concave graphene corner, as measured from six corners in the graphene vacancy island of Fig. 11.1E and F.

11.4 The influence of corner energy

A problem arose when the kink creation rate (unit/frame/site) was measured, as shown in Fig. 11.3. The local structure for a kink advance is very similar as kink creation at a 120° corner. But our counting shows that the kink creation rate for 120° is 0.28 ± 0.09 unit/frame/site, while the kink advance rate is 4.75 ± 0.4 unit/frame/site. Actually, it is faster than kink creation on a corner of any angle. This can be explained by the fact that the first kink created at the corner introduces two new corners for the advance of the kinks. This means the very detailed structure, in this case corner energy of graphene, has an influence on the growth.

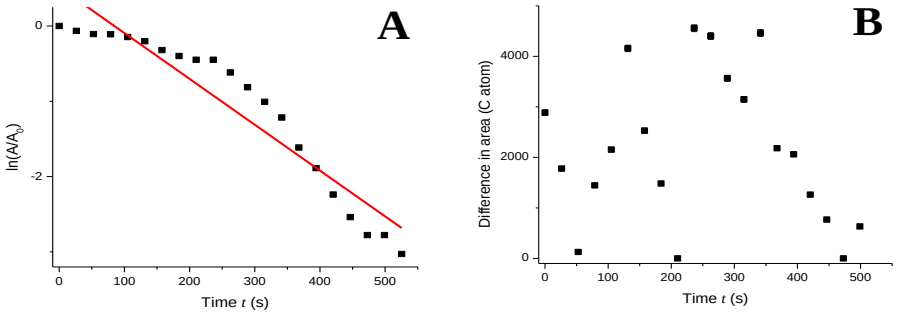

Fig. 11.4 (A) Semi-logarithmic plot of the time dependence of the area A of the enclosed Rh region in the episode between images C and D of Fig. 11.1. The linear fit to the logarithm of the area has a slope of -6.1 x 10^{-3} s^{-1}. (B) Difference in area between subsequent frames for the same episode. The error deriving from atom-by-atom statistics margins is within the symbol size.

11.5 Difference between growth at external and internal graphene edges

For the episode between panels A and B in Fig. 11.1, the average edge advancement rates $|dA/Ldt|$ of the four graphene islands and the one graphene vacancy island (labeled 1 to 5) were determined to be 1.9 ± 0.7, 0.2 ± 0.3, 1.7 ± 1.5, 3.2 ± 0.5, and 49 ±

27 pm/s respectively. In spite of the large error margins, we can draw two conclusions. Firstly, island 2 grew at a much lower rate than the others. In fact, the size of island 2 remained unchanged during the entire 865 s period that it was in view of the STM. Secondly, the edge of the vacancy island (labeled 5) advanced much more rapidly (more than 20 times) than the rest. As these have been truly simultaneous observations, with all island and vacancy structures exposed to equal ethylene fluxes, we assume that the concentrations of C adatoms near their edges should have been nearly equal. Therefore, we have to ascribe the differences in growth rate to differences in the edge configurations. The most important geometrical difference between graphene islands and vacancy islands within the graphene overlayer is that the contour of a vacancy island naturally contains concave corners (i.e. with angles below 180°), which can be of decisive importance. Adding the first new moiré unit requires the introduction of two new kinks along a straight step section, whereas it only requires a single kink at a concave corner. If we assume that the kink formation energy determines the rate at which new rows of moiré unit cells are initiated this rate should be significantly higher at concave corners than at straight steps or convex corners and, thus, there should be a large systematic difference in growth rate between graphene islands, with only straight steps and convex corners, and graphene vacancy islands, with primarily concave corners. This scenario also naturally explains why small graphene islands, such as island 2, grow even more slowly. To understand the latter observation, we assume that all graphene edges are populated by the same density S^{edge} of mobile C edge adatoms, in equilibrium with the C adatom density S on the surrounding metal substrate. The start of a new moiré unit cell requires the simultaneous presence of m C atoms, where m could be equal to the number $n = 5$, mentioned above. When the edge of the island is significantly shorter than am/S^{edge}, where a is the lattice constant of the graphene, the average number of C adatoms on the island edge is insufficient to get the process started, which leads to a significant suppression of the growth rate for the smaller islands. By contrast, the step advancement rate should be independent of size for the large graphene islands, as seems consistent with other work [98].

11.6 From which carbon does graphene grow?

Since the edge growth speeds were so different in Fig. 11.1, one may ask whether the edges were fed from the same source of carbon. As ethylene molecules only decompose on the bare Rh surface [51, 58], the carbon supply should become lower while the graphene coverage is increasing. In order to understand this, we first consider the assumption that in a graphene vacancy carbon adatoms cannot diffuse out of the enclosed Rh areas and the fraction of carbon escaping into the Rh substrate is negligible. Then, the total flux F of carbon atoms deposited on an enclosed Rh region should be simply proportional to the area A of this region, the impingement rate I of ethylene molecules, and the average number λ of carbon atoms deposited per impinging ethylene molecule. Since carbon is not accumulating in the enclosed area, e.g. in the form of new graphene nuclei, we can equate the flux of deposited carbon atoms to the rate at which the Rh area fills up with graphene:

$$\frac{dA}{dt} = -\frac{A}{D} I\lambda = \frac{A}{D}\lambda \frac{P}{\sqrt{2\pi m k_b T}} = -\alpha A P \lambda$$

Here, D represents the areal density of carbon atoms in the graphene overlayer and the impingement rate of ethylene I is expressed in terms of the ethylene gas pressure P, the (gas) temperature T, and the mass m of an ethylene molecule, using standard kinetic gas theory. The part that has surely remained unchanged during deposition has been combined in the constant α, which equals 7.5 x 10^4 $mbar^{-1}s^{-1}$ for ethylene gas at 293 K. Based on this differential equation, we expect exponential decay of the uncovered area:

$$\ln\left(\frac{A}{A_0}\right) = -\alpha P \lambda t \qquad \text{Eq. 11.2}$$

We have tested this in Fig. 11.4A by plotting the time dependence of the measured area of the enclosed Rh regions during the episode between Fig. 11.1C and D on a semi-logarithmic scale. From the slope of the straight-line fit in Fig. 11.4A, of -6.1 x 10^{-3} s^{-1}, and the ethylene pressures, we obtain an average value of λ=14. This λ-value suggests that each ethylene molecule that impinged on the Rh surface was accompanied by the addition of an average of 14 C atoms to the growing graphene layer. This greatly

exceeds the two C atoms in an ethylene molecule. Several sources of systematic error may have influenced the value of λ determined here. For example, the difference in position between the pressure gauge and the sample may have led to a systematic over- or under-estimate of the local pressure at the Rh substrate. Similarly, the presence of the STM tip may have reduced the ethylene pressure locally, precisely in the field of view of the STM. Whereas the tip-effect could only *reduce* the apparent λ, the geometry of our UHV system is such that the first effect cannot lead to an apparent *increase* of λ by more than a factor 2. Therefore, we are forced to conclude that the extra atoms must have come from the C that was dissolved in the Rh substrate during earlier stages of the deposition. The segregation of dissolved C adds a memory effect to the effective flux of C to the surface. In the early stages of graphene growth, the adatom density is high, resulting in a high rate of C dissolution. By contrast, the final stages, e.g. when the vacancy islands in the graphene are filling up, are characterized by much shorter adatom residence times and, hence, much lower adatom densities. During these stages, the dissolved C will partly re-surface and contribute to the growth rate of the graphene. We suggest that this effect is causing the high λ-value derived above.

11.7 Conclusion

In conclusion, we have shown that the moiré pattern plays an important role in the growth of graphene on Rh(111). Graphene has a preference to form complete moiré unit cells, which modulates the growth. After reaching the critical nucleus for the addition of one moiré unit, which we speculate to be a small number of added C atoms, the remaining atoms follow to quickly complete the rest of the moiré unit. By direct measurements of the rates at which moiré units are added at different sites we have drawn the following conclusions. Growth proceeds by kink creation and kink advancement, with kink creation being the rate limiting step. After a kink unit has been created on the edge of graphene, a full row of new moiré units quickly follows. It is easier to create a kink at concave corners of graphene. For this reason, the average growth rate in vacancy islands is much higher than that of compact islands. Because kink creation is the limiting step for graphene growth, differences in kink creation barrier also result in different C adatom densities during graphene growth, which has an effect on the flux of C dissolving into or segregating out of the Rh substrate.